Journal of Power Sources 196 (2011) 9585–9589

Contents lists available at ScienceDirect

Journal of Power Sources

journal homepage: www.elsevier.com/locate/jpowsour

Study on the structure and hydrogen absorption–desorption characteristics of as-cast and annealed $La_{0.78}Mg_{0.22}Ni_{3.48}Co_{0.22}Cu_{0.12}$ alloys

Taizhong Huang[a,b,d,*], Jitian Han[b], Yihe Zhang[c,d,**], Jiemei Yu[a,b], Guoxin Sun[a], Hao Ren[a], Xianxia Yuan[e]

[a] School of Chemistry and Chemical Engineering, University of Jinan, 106 Jiwei Road, Jinan, Shandong 250022, PR China
[b] School of Energy and Power Engineering, South Campus, Shandong University, No. 12793, Jingshi Road, Jinan, Shandong 250061, China
[c] Shandong Provincial Key Laboratory of Fluorine Chemistry and Chemical Materials, University of Jinan, 106 Jiwei Road, Jinan, Shandong 250022, PR China
[d] National Laboratory of Mineral Materials, School of Material Science and Technology, China University of Geosciences, Beijing 100083, China
[e] Department of Chemical Engineering, Shanghai Jiao Tong University, Shanghai 200240, China

ARTICLE INFO

Article history:
Received 10 May 2011
Received in revised form 26 June 2011
Accepted 7 July 2011
Available online 20 July 2011

Keywords:
Hydrogen storage alloy
Annealing treatment
X-ray diffraction
Pressure composition isotherm
Hysteresis

ABSTRACT

$La_{0.78}Mg_{0.22}Ni_{3.48}Co_{0.22}Cu_{0.12}$ alloy is one kind of nonstoichiometric $AB_{3.5}$ type hydrogen storage alloy with low cost and high capacity. In this paper, the effect of annealing treatment on the structure and hydrogen absorption–desorption characteristics of the alloy is discussed. The annealing temperature is determined by using thermogravimetry–differential scanning calorimetry (TG–DSC) tests. The structure of as-cast and annealed alloys is examined by X-ray diffraction (XRD) and scanning electron microscopy (SEM). XRD results show that the crystal cell volume decreases after annealing treatment. SEM tests reveal that the structure of the annealed alloys is more regular than that of the as-cast alloy. Influences of annealing treatment on maximum and reversible hydrogen storage capacity, hysteresis factor (H_f) between hydrogen absorption and desorption, sloping factor (S_f), enthalpy changes (ΔH) and entropy changes (ΔS) of hydrogen absorption are discussed in detail.

1. Introduction

Metal hydride is one of the most promising methods for hydrogen storage. Until now, many kinds of hydrogen storage alloys have been studied [1–6]. In order to improve the performance of hydrogen storage alloys, surface decoration, alkaline treatment, annealing treatment and other methods were developed [7,2,8]. In all of the developed methods, annealing treatment is one of the most widely employed. There are different opinions on the effect of annealing treatment on hydrogen storage alloys.

Zhu et al. studied the effect of annealing treatment on the cycling stability of hydrogen storage alloys [9,10]. Results showed that the discharge capacity, high rate discharge ability and cycle life of the alloys were improved by annealing treatment. The composition of the annealed alloy was more homogeneous than that of the as-cast alloy. The study of annealing treatment on Mg thin film drew similar conclusions. The structure of the annealed alloy was greatly influenced by annealing temperature [11]. The favorable morphology and structure induced by the annealing treatment improved hydriding kinetics of alloys. Pan and his coworkers also found that the discharge capacity and cycle life of $La_{0.7}Mg_{0.3}Ni_{2.45}Co_{0.75}Mn_{0.1}Al_{0.2}$ hydrogen storage alloy were improved by annealing treatment owing to the homogenization of composition [12]. The study of Talaganis on AB_5 alloys also drew similar conclusions that hydrogen absorption properties could be improved by annealing treatment [13,14]. Hydrogen absorption and desorption characteristics of alloys were determined by the phase compositions, which were greatly influenced by annealing treatment. Li and his coworkers studied the effect of annealing on structural and electrochemical properties of $(LaPrNdZr)_{0.83}Mg_{0.17}(NiCoAlMn)_{3.3}$ alloy. Results showed that the maximum electrochemical discharge capacity changed with annealing temperature [15].

LaMgNiCoCu based alloys showed good hydrogen absorption and desorption characteristics [16]. In this paper, the effect of annealing treatment on the structure and hydrogen absorption–desorption characteristics of nonstoichiometric $AB_{3.5}$ type $La_{0.78}Mg_{0.22}Ni_{3.48}Co_{0.22}Cu_{0.12}$ alloy are examined in detail.

2. Experimental

The purity of La, Ni, Co and Cu was all over 99.9 wt.%. Mg was used in the form of Mg–Ni binary alloys. The binary alloy was composed of Mg 40 wt.% and Ni 60 wt.%. $La_{0.7}Mg_{0.3}Ni_{3.2}Co_{0.22}Cu_{0.12}$

* Corresponding author at: School of Chemistry and Chemical Engineering, University of Jinan, 106 Jiwei Road, Jinan, Shandong 250022, PR China. Tel.: +86 531 82765955.
** Corresponding author at: Shandong Provincial Key Laboratory of Fluorine Chemistry and Chemical Materials, University of Jinan, 106 Jiwei Road, Jinan, Shandong 250022, PR China. Tel.: +86 10 82322759.
E-mail address: chm_huangtz@ujn.edu.cn (T. Huang).

0378-7753/$ – see front matter © 2011 Elsevier B.V. All rights reserved.
doi:10.1016/j.jpowsour.2011.07.038

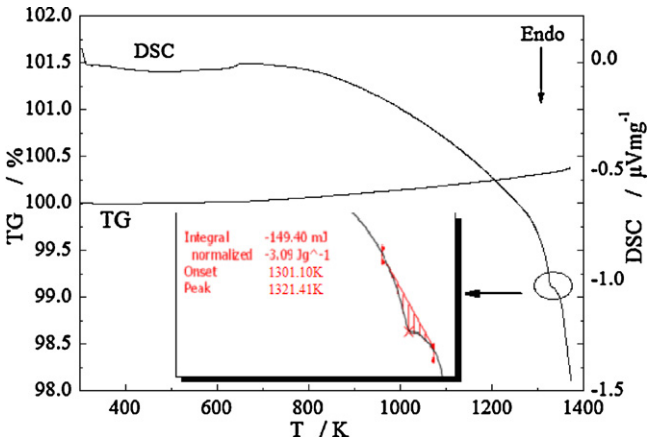

Fig. 1. TG–DSC testing results of as-cast $La_{0.78}Mg_{0.22}Ni_{3.48}Co_{0.22}Cu_{0.12}$ alloy.

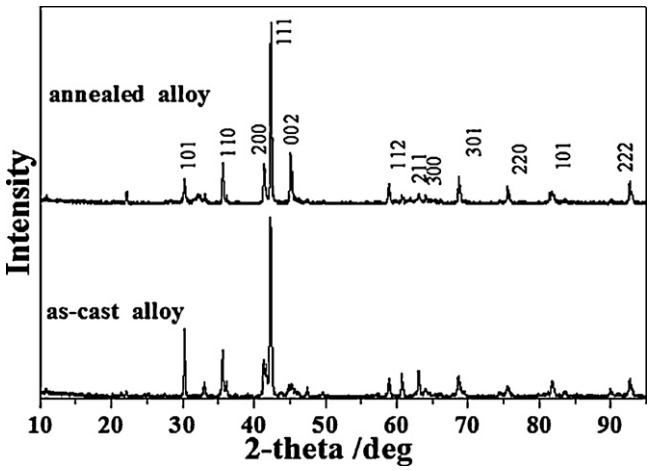

Fig. 3. XRD patterns of as-cast and annealed $La_{0.78}Mg_{0.22}Ni_{3.48}Co_{0.22}Cu_{0.12}$ alloy.

alloy was prepared by induction melting in a water-cooled copper crucible under the protection of argon atmosphere. Ingot was remelted three times to ensure the homogeneity of the alloy. Then the ingot was divided into two parts. One part was adopted in the as-cast state. Another part was prepared for annealing treatment. The annealing temperature was determined by thermo-gravimetry (TG) and differential scanning calorimetry (DSC) technology coupling thermal analyses using NETSCH STA 449C. 48.3400 ± 0.0001 mg as-cast alloys were employed in TG–DSC tests. The tests were conducted from 300 K to 1373 K with the heating rate of 20 K min^{-1}. High purity gas Ar was used as the carrier gas with the rate of 20 ml min^{-1}. The results are shown in Fig. 1.

Fig. 1 clearly shows that no mass losses could be detected by TG testing results. The insert diagram revealed that a peak appeared at 1321.41 K, which should be in corresponding with the structure changes of the alloy. So the annealing temperature was ascertained at 1325 K. To ensure the structure changes could be fully conducted, the ingot was kept 6 h at 1325 K under the protection of argon atmosphere.

Then both as-cast and annealed alloys were fully crushed and the powders were sieved through 200 meshes for X-ray powder diffraction (XRD) tests, separately. XRD tests were conducted by using an X'Pert-MPD instrument (graphite filtered Cu K_α radiation). The scanning speed was 5 degree per minute in a step of 0.02 degree from 10 degree to 95 degree.

SEM tests were conducted by using a Quanta 3D FEG scanning electron microscope (FEI Company) with charges of 15 kV and 10 pA.

Pressure composition isotherm (PCT) tests were conducted by using a gas reaction controller, which is a product of Advanced Materials Corporation, USA. Three grams of each sample were put into the instrument and fully activated. Then PCT tests were performed at different temperatures. Hydrogen gas with purity over 99.9999% was supplied from a cylinder.

3. Results and discussion

3.1. SEM tests

SEM results of both as-cast and annealed $La_{0.78}Mg_{0.22}Ni_{3.48}Co_{0.22}Cu_{0.12}$ alloys are shown in Fig. 2. It is clearly seen that the structure of the annealed alloy is more regular than that of as-cast alloy. Similar conclusions were also drawn in the study of annealing effect on hydrogen storage of Mg thin film [11]. The structure of the alloy was homogenized by the annealing treatment.

3.2. XRD results

XRD patterns of the as-cast and annealed $La_{0.78}Mg_{0.22}Ni_{3.48}Co_{0.22}Cu_{0.12}$ alloys are displayed in Fig. 3. From the XRD patterns, it was confirmed that single $La_{0.98}Ni_{5.03}$ phase (hexagonal structure, space group P6/mmm, JCPDS No. 65-3849) existed in both the as-cast alloy and the annealed alloy. Corresponding XRD diffraction peaks of annealed alloy were sharper than that of as-cast alloy, which illustrated that the

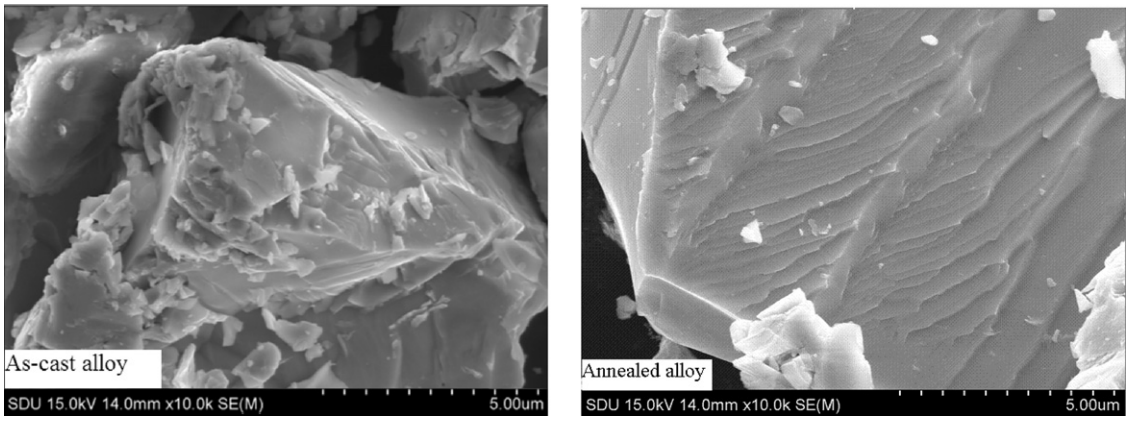

Fig. 2. SEM testing results of as-cast and annealed $La_{0.78}Mg_{0.22}Ni_{3.48}Co_{0.22}Cu_{0.12}$ alloys.

Table 1
Crystal cell parameters *a*, *c* and *V* of as-cast and annealed $La_{0.78}Mg_{0.22}Ni_{3.48}Co_{0.22}Cu_{0.12}$ alloy.

	a (Å)	*c*(Å)	*V* (Å^3)
As-cast	5.028	3.990	87.354
Annealed	4.997	3.987	86.215

structure of annealed alloy was more homogeneous than that of as-cast alloy. The phase composition and corresponding crystal cell parameters were calculated using the software of Jade 5.0. The obtained results are shown in Table 1.

It could be seen from Table 1 that the crystal cell parameters of the annealed alloy were smaller than those of the as-cast alloy. In the research of $(LaPrNdZr)_{0.83}Mg_{0.17}(NiCoAlMn)_{3.3}$ alloy, it was also found that the crystal cell volume decreased after annealing treatment [15]. But researches on BCC solid solution $(Ti_{0.8}Zr_{0.2})(V_{0.533}Mn_{0.107}Cr_{0.16}\ Ni_{0.2})_4$ alloy drew different conclusions that the crystal cell parameters increased upon annealing treatment [17]. The structure changes of alloys during annealing treatment were influenced by both annealing temperature and alloy compositional elements. The enlargement should be caused by the substitution of Zr for Ti. The radius of Zr atom is bigger than that of Ti atom. The phase composition of $La_{0.78}Mg_{0.22}Ni_{3.48}Co_{0.22}Cu_{0.12}$ alloy is $La_{0.98}Ni_{5.03}$ phase. The low stoichiometric alloy resulted in the existence of lattice strain and crystal defects in the as-cast alloy. So the decrease of crystal cell parameters may be caused by the annihilation of lattice strain and crystal defects during annealing treatment. In the research of annealing effect on $LmNi_{3.65}Al_{0.34}Mn_{0.27}Co_{0.74}$ alloy, the changes of crystal cell parameters were attributed to the annihilation of lattice strain and crystal defects during annealing process [18].

3.3. PCT measurements

PCT measurements of the as-cast and annealed alloys are shown in Fig. 4. Based on these tests, the maximum hydrogen storage capacity (C_{max}) and the hydrogen absorbing plateau pressure (P) at different temperatures could be obtained. Reversible hydrogen storage capacity (C_{rev}), which is defined as the differences of the maximum hydrogen storage capacity and the residue capacity at the end of hydrogen desorption, were calculated. The results are shown in Table 2.

Table 2 clearly revealed that, for each alloy, the C_{max} and C_{rev} decreased with the increasing temperature. Similar phenomena were also observed in the research of AB_5 type alloys [14].

It could also be seen from Table 2 that the C_{rev} of the annealed alloy was higher than that of the as-cast alloy at the same temperature. Annealing treatment improved the reversible hydrogen storage capacity of the alloy. In the study of the annealing effects on $LmNi_{3.65}Al_{0.34}Mn_{0.27}Co_{0.74}$ alloy, it had also been found that the maximum hydrogen storage capacity slightly increased after annealing treatment [18]. This should be attributed to the annealing treatment, which homogenized the structure. The C_{max} of the as-cast alloy was higher than that of the annealed alloy at 273 K and 303 K, but lower than that of annealed alloy at 333 K and 353 K. This maybe caused by the changes of crystal cell volume. As discussed in Section 3.2, the crystal cell volume of the as-cast alloy was bigger than that of the annealed alloy. So the C_{max} of the as-cast alloy was higher than that of the annealed alloy.

Table 2
C_{max} C_{rev} and P of as-cast and annealed $La_{0.78}Mg_{0.22}Ni_{3.48}Co_{0.22}Cu_{0.12}$ alloys at different temperatures.

T (K)	As-cast alloy			Annealed alloy		
	C_{max} (wt.%)	C_{rev} (wt.%)	*P* (atm)	C_{max} (wt.%)	C_{rev} (wt.%)	*P* (atm)
273	1.69	1.50	0.571	1.62	1.53	0.864
303	1.79	1.52	1.316	1.61	1.54	2.584
333	1.58	1.43	5.983	1.61	1.50	6.87
353	1.52	1.38	10.56	1.55	1.44	11.745

It could also be seen from Table 2 that the hydrogen absorbing plateau pressure of the annealed alloy was higher than that of the as-cast alloy. This should be caused by the decrease of crystal cell volume. Hydrogen absorbing pressure was elevated by the decreased crystal cell volume. Similar phenomenon was also observed in the research of $La_{2-X}Ti_XMgNi_9$ alloys [19]. The expansion of cell volume leads to a decrease of plateau pressure. On the other hand, the hysteresis also has influences on hydrogen absorption and desorption. The influences will be discussed later.

3.4. Enthalpy changes and entropy changes of hydrogen absorption

The heat formation during the course of hydrogen absorption could be evaluated according to PCT tests at different temperatures. The enthalpy changes (ΔH) and entropy changes (ΔS) of hydrogen absorption were calculated according to Van't-Hoff equation $\ln P = -(\Delta H/RT) + (\Delta S/R)$ [20]. ΔH and ΔS of hydrogen absorption could be obtained by the slope and intercept of fitting line. The fitting line for ΔH and ΔS of hydrogen absorption of the as-cast and annealed $La_{0.78}Mg_{0.22}Ni_{3.48}Co_{0.22}Cu_{0.12}$ alloys are illustrated in Fig. 5. The calculated ΔH and ΔS are displayed in Table 3. Table 3 clearly shows that the enthalpy changes and entropy changes of hydrogen absorption of the annealed alloy were lower than that of as-cast alloy. This should be attributed to the homogenized struc-

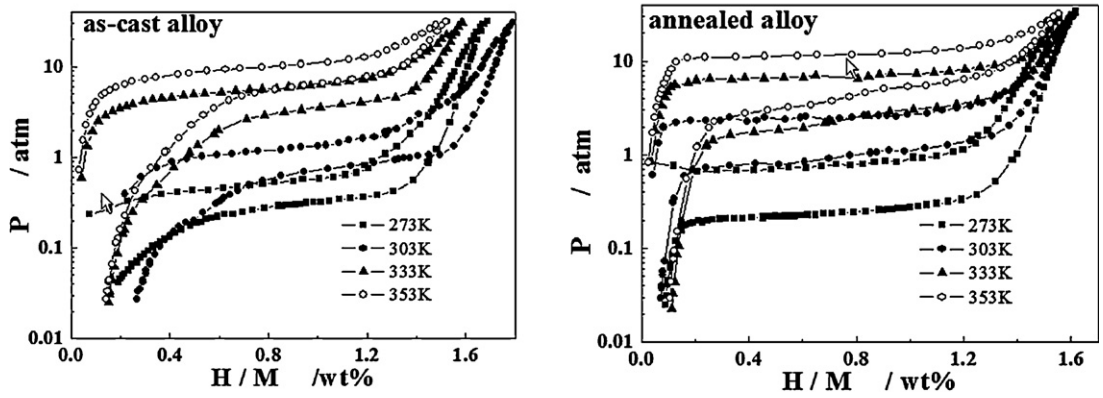

Fig. 4. PCT testing results of as-cast and annealed $La_{0.78}Mg_{0.22}Ni_{3.48}Co_{0.22}Cu_{0.12}$ alloys.

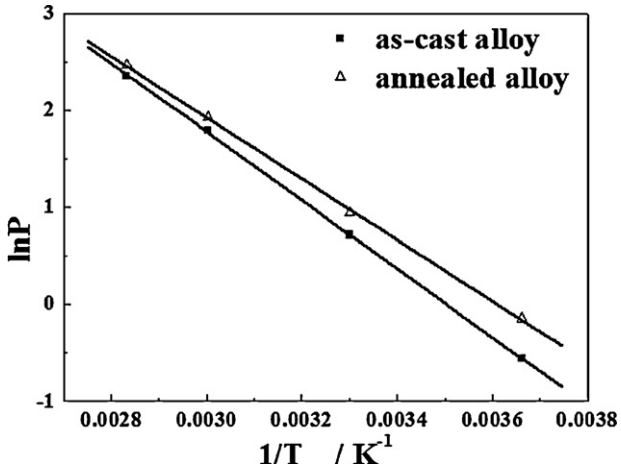

Fig. 5. Fitting line for ΔH and ΔS of hydrogen absorption.

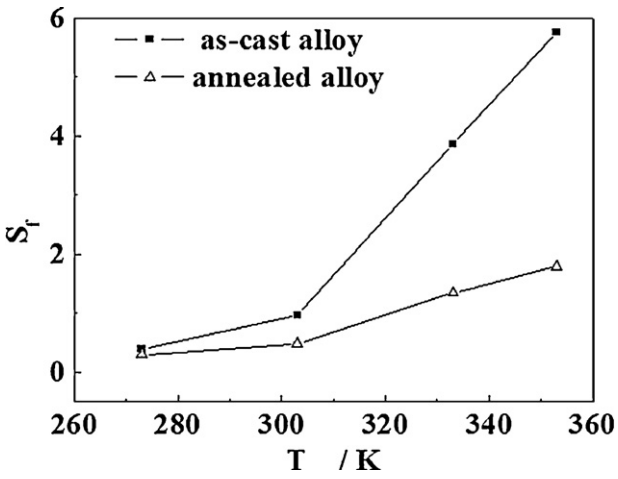

Fig. 7. S_f of as-cast and annealed alloys at different temperatures.

Table 3
ΔH and ΔS of hydrogen absorption of as-cast and annealed alloys.

Alloy	ΔH (kJ mol^{-1})	ΔH (J mol^{-1} K^{-1})
As-cast	29.5	103.3
Annealed	26.2	94.7

ture. Annealing treatment decreased the enthalpy changes and entropy changes of hydrogen absorption.

3.5. Influences of annealing on H_f

Reversibility between hydrogen absorption and desorption is an important performances for the practical application of hydrogen storage alloys. Hydrogen storage alloy with high performance should possess a good reversibility. Hysteresis factor (H_f), which is defined as $H_f = \ln(P_{abs}/P_{des})$, is usually employed to evaluate the reversibility between hydrogen absorption and desorption [21]. P_{abs} and P_{des} are hydrogen pressure corresponding to hydrogen absorption and desorption, respectively, at certain hydrogen storage capacity. In this paper, P_{abs} and P_{des} corresponding to the capacity of $H/M = 0.9$ were adopted. The calculated H_f of both as-cast and annealed alloys at different temperatures are presented in Fig. 6.

It is clearly observed from Fig. 6 that H_f of as-cast and annealed alloys decreased with increasing temperature. In the study of annealing effect on hydrogen absorption and desorption performances of milled AB_5 type alloys, it was also found that H_f decreased with the increase of testing temperature [14]. Hydrogen desorption is an endothermal process. On the other hand, the increasing temperature also promoted the activity of hydrogen storage alloys. So the reversibility between hydrogen absorption and desorption was improved by the increasing temperature and eventually resulted in the decrease of H_f.

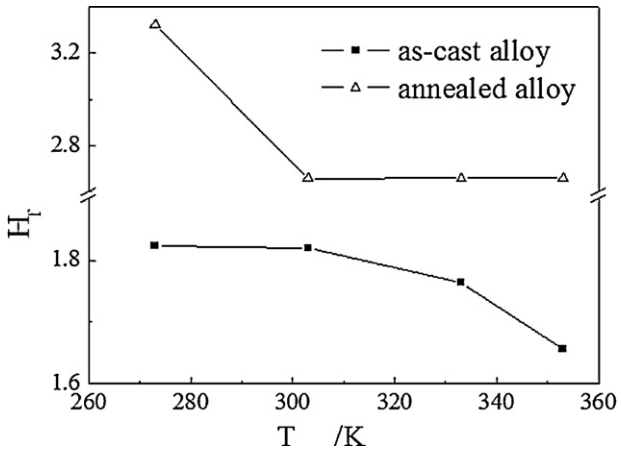

Fig. 6. H_f of as-cast and annealed alloys at different temperatures.

It could also be seen from Fig. 6 that H_f of the annealed alloy was higher than that of as-cast alloy at the same temperature. As discussed in Section 3.3, the plateau pressure of hydrogen absorption of annealed alloy was higher than that of as-cast alloy. On the other hand, it could also be seen from Fig. 4 that the plateau pressure of hydrogen desorption of the annealed alloy was lower than that of the as-cast alloy. So H_f between hydrogen absorption and desorption of annealed alloy was higher than that of as-cast alloy. This should be caused by the decrease of crystal cell volume. The deceased crystal cell volume elevated the pressure of hydrogen absorption and decreased that of hydrogen desorption. Annealing treatment resulted in the increase of H_f between hydrogen absorption and desorption.

3.6. Influences of annealing on S_f

Sloping factor (S_f) was employed to elucidate the plateau performance of hydrogen absorption. S_f is defined as $S_f = (P_1 - P_2)/((H/M)_1 - (H/M)_2)$, where P_1 and P_2 were the pressure of hydrogen corresponding to the hydrogen storage capacity of $(H/M)_1$ and $(H/M)_2$, respectively [22]. In this paper, the pressure of hydrogen absorption corresponding to $H/M = 0.4$ and $H/M = 1.0$ were adopted. S_f of hydrogen absorption of both as-cast and annealed alloys at different temperatures is illustrated in Fig. 7.

It could be seen from Fig. 7 that S_f of hydrogen absorption of both as-cast and annealed alloys was enhanced with the increase of testing temperature, which meant that the plateau performance of hydrogen absorption was weakened. This was in consistent with PCT testing results that the plateau length of hydrogen absorption shortened with increasing temperature.

Fig. 7 also revealed that S_f of hydrogen absorption of the annealed alloy was lower than that of the as-cast alloy at the same testing temperature, which meant that annealing treatment improved the hydrogen absorbing plateau performance. Researches on $(LaPrNdZr)_{0.83}Mg_{0.17}(NiCoAlMn)_{3.3}$ alloy also showed that the annealing treatment decreased S_f of hydrogen absorption [15]. This should be ascribed to the homogeneous hexagonal structure [18]. S_f of the annealed $La_{0.67}Mg_{0.33}Ni_{2.5}Co_{0.5}$ alloy was also lower than that of the as-cast alloy [23]. H_f and S_f

of hydrogen absorption and desorption were greatly influenced by annealing treatment [24]. The homogeneous composition and perfected structure improved the plateau performance of hydrogen absorption.

4. Conclusions

This paper mainly discussed the influences of annealing treatment on the structure and hydrogen absorption–desorption characteristics of $La_{0.78}Mg_{0.22}Ni_{3.48}Co_{0.22}Cu_{0.12}$ alloy. Based on the tests and discussions, conclusions could be drawn as follow:

(1) The crystal cell volume of the alloy decreased after annealing treatment.
(2) The plateau performance of hydrogen absorption and desorption was improved by annealing treatment.
(3) Enthalpy changes and entropy changes of hydrogen absorption of the annealed alloy were lower than that of as-cast alloy.
(4) The reversible hydrogen storage capacity of annealed alloy was higher than that of as-cast alloy at the same temperature.

Acknowledgements

This work was supported by National “863” Program of China (Grant No. 2007AA05Z149), Research Fund of Jinan University (Grant No. XKY 0805) and the Scientific Research Foundation for the Returned Overseas Chinese Scholars, State Education Ministry, China, Open Fund of National Laboratory of Mineral Materials (No. 09B004) and China Postdoctoral Science Foundation funded project, the National Natural Science Foundation of China (No. 51074078), University Science Development Project of Shandong Provincial (No. J11LD02).

References

[1] T. Kohno, H. Yoshida, F. Kawashima, T. Inaba, I. Sakai, M. Yamamoto, M. Kanda, J. Alloys Compd. 311 (2000) L5–L7.
[2] T. Bai, S. Han, X. Zhu, Y. Zhang, Y. Li, W. Zhang, Mater. Chem. Phys. 117 (2009) 173–177.
[3] R. Tang, Y. Liu, C. Zhu, J. Zhu, G. Yu, Intermetallics 14 (2006) 361–366.
[4] T. Huang, Z. Wu, B. Xia, T. Huang, Mater. Chem. Phys. 93 (2005) 544–547.
[5] B. Sakintuna, F. Lamari-Darkrim, M. Hirscher, Int. J. Hydrogen Energy 32 (2007) 1121–1140.
[6] S.L. Li, P. Wang, W. Chen, G. Luo, D.M. Chen, K. Yang, J. Alloys Compd. 485 (1-2) (2009) 867–871.
[7] M. Raju, M.V. Ananth, L. Vijayaraghavan, J. Alloys Compd. 475 (2009) 664–671.
[8] C.-H. Chen, C.-C. Huang, Int. J. Hydrogen Energy 32 (2007) 237–246.
[9] Y. Zhu, H. Pan, M. Gao, Y. Liu, Q. Wang, J. Alloys Compd. 347 (2002) 279–284.
[10] Y. Zhu, H. Pan, M. Gao, Y. Liu, Q. Wang, J. Alloys Compd. 348 (2003) 301–308.
[11] J. Qu, Y. Wang, L. Xie, J. Zheng, Y. Liu, X. Li, Int. J. Hydrogen Energy 34 (2009) 1910–1915.
[12] H. Pan, N. Chen, M. Gao, R. Li, Y. Lei, Q. Wang, J. Alloys Compd. 397 (2005) 306–312.
[13] B.A. Talaganis, M.R. Esquivel, G. Meyer, J. Alloys Compd. 495 (2010) 541–544.
[14] B.A. Talaganis, M.R. Esquivel, G. Meyer, Int. J. Hydrogen Energy 34 (2009) 2062–2068.
[15] F. Li, K. Young, T. Ouchi, M.A. Fetcenko, J. Alloys Compd. 471 (2009) 371–377.
[16] T. Huang, Z. Wu, J. Han, G. Sun, J. Yu, X. Cao, N. Xu, Y. Zhang, Int. J. Hydrogen Energy 35 (2010) 8592–8596.
[17] Y. Zhu, H. Pan, M. Gao, Y. Liu, Q. Wang, Int. J. Hydrogen Energy 28 (2003) 389–394.
[18] H.C. Lin, K.M. Lin, H.T. Chou, M.T. Yeh, J. Alloys Compd. 358 (2003) 281–287.
[19] W. Jiang, Z. Lan, L. Xu, G. Li, J. Guo, Int. J. Hydrogen Energy 34 (2009) 4827–4932.
[20] K. Doi, S. Hino, H. Miyaok, T. Ichikawa, Y. Kojima, J. Power Sources 196 (2011) 504–507.
[21] T. Huang, W. Zhu, X. Yu, J. Chen, B. Xia, T. Huang, N. Xu, Intermetallics 12 (2004) 91–96.
[22] S.L. Li, P. Wang, W. Chen, G. Luo, D.M. Chen, K. Yang, Int. J. Hydrogen Energy 35 (2010) 3537–3545.
[23] F. Zhang, Y. Luo, J. Chen, R. Yan, L. Kang, J. Chen, J. Power Sources 150 (2005) 247–254.
[24] Z. Zhou, Y. Song, S. Cui, C. Huang, W. Qian, C. Lin, Y. Zhang, Y. Lin, J. Alloys Compd. 501 (2010) 47–53.